SHIFTED-EXCITATION RAMAN SPECTROSCOPIC METHODOLOGIES DEVELOPED FOR THE COMPACT INTEGRATED RAMAN SPECTROMETER (CIRS) J. L. Lambert[1], Alian Wang[2], and J.B. Cooper[3] [1]Jet Propulsion Laboratory, California Institute of Technology, james.l.lambert@jpl.nasa.gov, [2]Washington University in St. Louis, [3]Old Dominion University.

Introduction: Laser induced fluorescence (LIF) spectroscopy and laser Raman spectroscopy (LRS) reveal information about a compound's electronic and molecular structure and therefore represent powerful tools for planetary science investigations. However in some terrestrial samples, the raw spectra acquired from a Raman instrument may contain LIF components that can, along with their associated shot noise, obscure much weaker Raman spectral signatures. Therefore during the development of a laser Raman system for planetary exploration, we need to find the answers for two relevant questions: (1) Will LIF be an important threat in Raman investigation of extraterrestrial samples? (2) What would the best methodology and philosophy to reduce the interference in case that fluorescence does occur? Supported by NASA MATISSE program, we are developing a Compact Integrated Raman Spectrometer (CIRS), seeking these answers is among the tasks of CIRS project.

Based on two sets of observations, we conclude that LIF would not be a major threat for LRS that uses cw green laser excitation for planetary explorations. One set of observations was made on Mars, by Optical Microscopy on Phoenix lander [1] and by MAHLI on Curiosity rover [2], where no obvious evidence of UV (365 nm) stimulated fluorescence from martian soils and martian rock targets were seen. The second set of observations was made on martian meteorites (Lafeyette, Nakhla, Zagami, EETA789001, Los Angeles, MIL03346, Tissint), lunar rock (75075,154), carbonaceous chondrites (Allende, Murchson, Tagish lake), and a set of L-, LL-, H-type meteorites, by UV-fluorescence imagery and/or by LRS using cw green laser excitation, the similar results were obtained in all these extraterrestrial materials [3-17].

These results confirm the feasibility for using the most simple and the optically most effective instrument configuration of LRS to accomplish its main goal, the definitive characterization of molecular species in planetary materials. It is the design philosophy of CIRS, i.e., to use the most mature technology (cw 532 nm laser, visible optics, CCD) to conduct autonomous robotic measurements on hundreds spots per sample during a planetary mission.

On the other hand, some extraterrestrial materials are found containing organic species. In addition, the sign of life may still exist on Mars. Some of these species will generate LIF in localized small spots in a sample during a CIRS line scan. For these spots, CIRS has two capabilities in its design to deal with: (1) detection of green-yellow-red fluorescence, stimulated by the 532 nm laser radiation, in the form of a Raman spectral background that provides knowledge of the central wavelength of broad fluorescence bands; and (2) imaging of green-blue fluorescence (stimulated by the UV LEDs in CIRS-Compact Imager function), providing knowledge of its spatial distribution in a 3×12 mm area.

Furthermore, Shifted Excitation Raman Difference Spectroscopic methodologies will be used to extract Raman spectroscopic molecular information from a strongly fluorescent sampling spot, which is the topic of this report. We performed experiments using a temperature tunable diode pumped solid-state (DPSS) laser in conjunction with a Raman microscope to implement both Shifted Excitation Raman Difference Spectroscopy (SERDS) and Serially Shifted Excitation (SSE). SERDS and SSE results are experimentally compared to determine the degree to which these methods mitigated detector fixed pattern noise, other background artifacts and LIF in Raman spectra of polycyclic aromatic hydrocarbons (PAHs) and mineral samples with significant levels of background fluorescence.

SERDS: LIF emission spectra can interfere with Raman spectra since the fluorescence cross-sections of many molecules can exceed Raman cross-sections by orders of magnitude. However, one implication of Kasha's rule [18] is that fluorescence emission spectra are independent of the excitation wavelength. This often, but not always, occurs since molecules excited into upper excitation states tend to relax non-radiatively into the lowest excited state. Therefore if a pair of spectra is acquired using slightly different excitation wavelengths, the resulting fluorescence emission spectra are nearly identical, while the Raman spectra are shifted with respect to one another in wavelength. In employing SERDS, the two spectra acquired are subtracted from one another with the goal of removing the fluorescence signature from the result while preserving a Raman difference signature. The SERDS-derived Raman difference spectrum can be re-integrated to reconstruct the original Raman spectrum with a reduced fluorescence baseline [19].

SSE: Spectra acquired using a laser excitation source that is serially tuned to three or more output frequencies can be processed to separately solve for the Raman and fluorescence spectral contributions to the raw spectral signature. SSE relies on a matrix-vector formulation that can be iteratively solved for

both the fluorescence and Raman vector components by employing the Lucy-Richardson algorithm [20]. While Lucy-Richardson matrix-vector operations can be quite computationally intensive, a more efficient means of implementing the algorithm was developed by Cooper and his collaborators [21].

Temperature tuning of a green DPSS Laser: We used a JDSU model CDPS532M laser, developed for CIRS, as the tunable excitation source for our SERDS and SSE experiments. The JDSU laser uses Nd:YVO_4 as the lasing medium optically pumped by a laser diode operating nominally at a wavelength of 808nm. The Nd:YVO_4 crystal, whose pump face is coated to be reflective at 1064 nm, combined with a spherically shaped output coupling mirror together form a hemispherical laser cavity.

A Potassium Titanyl Phosphate (KTP) crystal is mounted inside the cavity for frequency doubling the output frequency. The pump beam is linearly polarized, and the Nd:YVO_4 crystal is oriented such that its 1064 nm output is also linearly polarized. Since the KTP crystal is birefringent, it induces a directionally dependent polarization rotation of the light passing back and forth through the cavity. In order for lasing to occur, for a given mode, the polarization of the light leaving and returning to a given cavity mirror must be the same. Since the extraordinary and ordinary indices of refraction of the KTP crystal are functions of wavelength and each longitudinal mode has a different frequency, KTP severely constrains the number of longitudinal modes that satisfy this condition. The KTP crystal thereby reduces the number of possible lasing modes (often to just one), facilitating single frequency operation. The effect imposed by KTP inside the laser is well known, and is effectively a first-order Lyot filter, which has a sinusoidally shaped transmission function [22]. Since the indices of refraction of KTP are temperature dependent, the phase of the sinusoidal transmission function changes with temperature, allowing the laser to be tuned to a single frequency [23].

Regulation of the temperature of the laser's copper structure was performed with a thermoelectric cooler (TEC) with feedback provided by a thermistor mounted in the structure. Precise control of the laser's temperature provided a means to stabilize the laser's output frequency to specific set point values. In order to control the laser's frequency as required for our experiments, we removed the commercial electronics supplied with the laser and in its place used a Vuemetrix DPSS 4.0 controller. This controller allowed us to regulate both the laser's temperature and optical output power. Feedback proportional to the laser output power was provided by a pickoff beamsplitter and photodiode integrated with the laser head.

Figure 1 shows the set of laser excitation frequencies used in our experiments. Laser frequency varied periodically with temperature and was measured using a Bristol laser spectrum analyzer. Operating temperatures were avoided where two of the peaks of the Lyot filter's sinusoidal filter appeared under the Nd:YVO_4 crystal's gain profile as they caused dual frequency output. Additionally, temperature set points were carefully established to generate laser output frequencies that were as equally spaced as possible (~1cm^{-1} in this case) to facilitate processing by the SSE algorithm[21]. Raw spectra acquired using excitation wavelength pair were used to generate SERDS results.

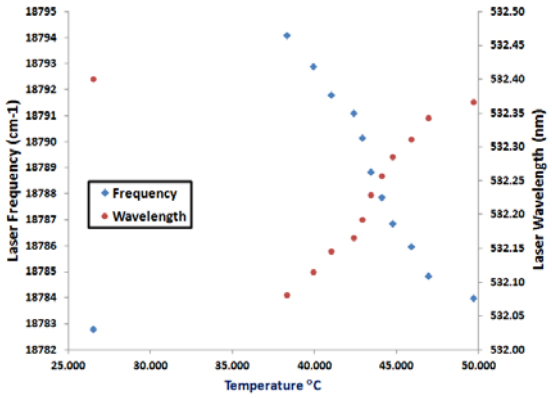

Figure 1: Laser output frequency and wavelength vs temperature

Raman Spectrometer used: A Kaiser Holospec f/1.8 Raman spectrometer with a dual blaze holographic grating, a 532nm notch filter, a 50 micron wide slit, and an Andor iDUS camera was used in our experiments. The Andor camera includes a four stage TEC cooler which was set to maintain the temperature of the CCD at -70°C during acquisition. A trigger output signal from the Andor camera was used to drive a shutter (Vincent Associates) to block the laser beam from the sample when the system was idle to minimize sample photobleaching. The excitation laser was fiber-coupled to a Kaiser Mark II probehead which was mounted in an Olympus BX60 Optical Microscope with a 10X (NA=0.22) objective. A graded-index multi-mode collection fiber was used to direct the collected light to the spectrometer. The instrument provided a free spectral range covering 200 cm^{-1} – 4000 cm^{-1} with a nominal resolution of 8 cm^{-1}.

Spectral Acquisition: The Vuemetrix controller was used regulate the temperature of the laser's TEC to within 0.10°C as well as maintain the laser output power at a constant level. One of the samples tested is Fluoranthene ($C_{16}H_{10}$), a highly fluorescent polycyclic aromatic hydrocarbon identified within carbonaceous chondrites including Murchinson, Cold Bokkeveld,

Yamato-791198 and Yamato-74662 [24]. Each spectrum was acquired with an integration time of 2s with 25 mW of incident laser power at each of the laser excitation frequencies shown in Figure 1.

Preprocessing: Figure 2A shows that the raw spectra acquired have similar shapes but with some variations in spectral intensity across the various runs conducted. Photobleaching from prior exposures and other experimental variability could account for this.

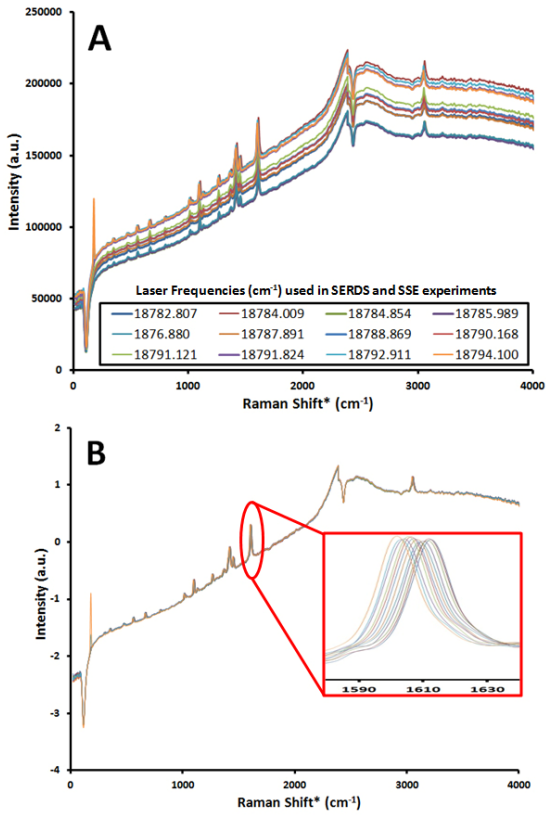

Figure 2: (A) Raw Spectra (12) of Fluoranthene (B) SNV Processed Spectra of Fluoranthene

To minimize the effects of these variations, standard normal variance (SNV) normalization [25] was applied prior to SERDS or SSE processing with to remove background fluorescence. The SSV processed dataset is shown in Figure 2B. As can be seen, SNV preserves the information content, including shifts induced by the changes in excitation wavelength (see Figure 2B inset), while providing a relatively common baseline across the different runs.

SERDS and SSE Processing: Raw and SERDS difference spectra for Fluoranthene with excitation frequencies pairs separated 8cm^{-1} separation is shown in Figure 3. Note the stitching artifact in the 2200cm^{-1} region resulting from joining spectra acquired from the two vertically displaced regions of the CCD is mostly removed through SERDS processing since it does not shift with wavelength.

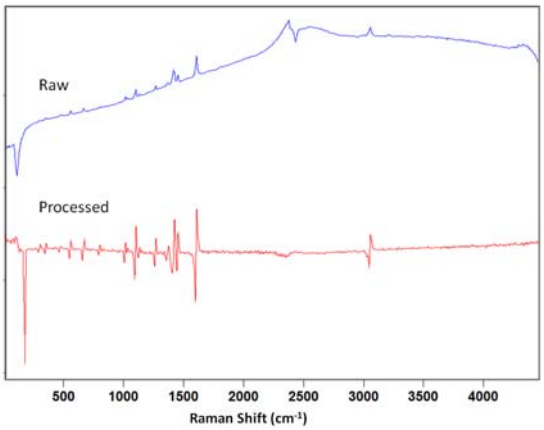

Figure 3: Laser output frequency and wavelength vs temperature

A raw and SSE spectrum processed for the same fluoranthene sample is shown in Figure 4. We iteratively processed a set of raw spectra acquired at 12 different excitation frequencies to obtain the SSE Raman solution vector using the method published by Cooper et. al[21].

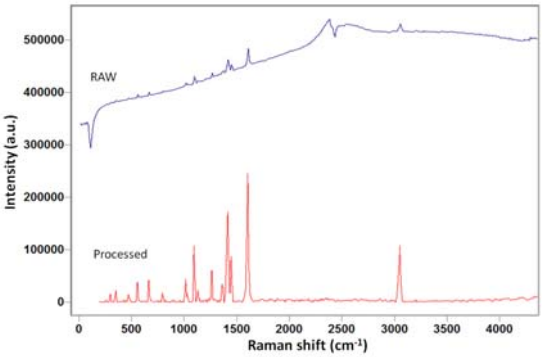

Figure 4: Fluoranthene spectra before and after SSE processing.

Discussion: The intracavity KTP crystal provides a convenient tool for temperature tuning the laser based on the Lyot filter effect for implementing both SERDS and SSE methods. Although we controlled the temperature of the laser in bulk with a single TEC, more rapid tuning of the laser could be realized by independently controlling the temperature of the KTP crystal itself. Additionally, separate temperature control of the KTP crystal could eliminate thermally induced changes in the host crystal's fluorescence emission spectrum and the pump laser output wavelength.

SERDS provides an effective means of eliminating fixed pattern noise and some fluorescence baseline effects. However, shot noise is increased as a result of subtracting a pair of spectra. Acquisition of SERDS spectra does allow one to discriminate between nar-

rowband fluorescence peaks from Raman peaks and this has utility in certain situations.

For fluorescence suppression SSE excitation is a more powerful tool than SERDS while imposing operational costs of needing to acquire spectra at additional excitation frequencies and with added computational load of iteratively computing the Raman signature. However, the technique *reduces* the shot noise due to fluorescence in the computed Raman spectra since shot noise is largely excluded from a solution derived from shifted spectral components of the observed spectra. In fact, it can be shown that if the total energy of exposure is kept constant, as the number of laser frequencies used in SSE is increased, that the SNR of the SSE processed Raman solution increases [26]

Conclusion: We have demonstrated that both SSE and SERDS methodologies work on fluorescent samples utilizing a cw green laser developed for CIRS. SERDS and SSE have generated high quality data for mineralogical analysis as well as organic detection, both are extremely important in planetary exploration. In the context of a flight instrument, both SERDS and SSE post-processing could be performed on the ground during mission operations. Accordingly, we are integrating SERDS and SSE protocols into CIRS, the LRS unit that we are developing for future planetary missions under MatISSE support.

Acknowledgements: This work has been funded by NASA's MatISSE program NNX13AM22G, and by efforts at the Jet Propulsion Laboratory, California Institute of Technology performed under contract with the National Aeronautics and Space Administration.

References: [1] Goetz, W., et al., (2012), Planetary and Space Science, V70, P134-147. [2] Minitti et al., (2014) abstract #2029 for 44th LPSC. [3] Wang et al., (2003), abstract #1753, 34th LPSC.[4] Minitti and McCoy (2012), abstract #2349 for 43rd LPSC; [5] Wang et al., 1995, JGR, 100, 21189-21199; [6] Haskin et al., 1997, JGR, 102, 19293-19306; [7] Korotev et al., 1998, LPSC, abs#1797; [8] Wang et al., 1999, JGR, 104, 8509–8519; [9] Wang et al., 2004, JRS, 35, 504-514; [10] Wang et al., 2004, Am. Minerals. 89, 665-680; [11] Kong et al., 2010, LPSC, abs# 2730; [12] Ling et al., 2011, ICARUS, 211, 101-113; [13] Takir et al., 2013, MPS, doi: 10.1111/maps.12171; [14] Haenecour et al., 2014, 11th GeoRaman, abs #5017; [15] Ling et al., 2014, 11th GeoRaman, abs#5089; [16] Wang et al., 2014, PSS; [17] Wei et al., 2014, this volume. [18] P. Klan, J. Wirtz (2009) Wiley: Hoboken, NJ [19] M. da Silva Martins, et. al (2010) Biomedical Optics Express 1, No 2, 617-626. [20] S.T. McCain et al. (2008) Optics Express 16, 10975-10991. [21] J.B. Cooper et al. (2013) Appl. Spectr. 67, 973-84. [22] J.Z. Sotor et al. (2011) Appl. Phys B 103, 67-74. [23] J.Z. Sotor et al. (2010) Opto-electr Rev 18, 75-79. [24] M. Sephton (2002) Nat. Prod. Rep. 19, 292-311. [25] R. Barnes, et. al (1989) Applied Spectroscopy 43, 772-777. [26] R. Willett (2007) ICASSP Vol 3, 833-840.